Supplementary Information for Effect of sound wall-vegetation combination barriers on pollution dispersion from freeways under early morning conditions

Dilhara Ranasinghe[1], Eon S. Lee[2], Yifang Zhu[2], Isis Frausto-Vicencio[1], Wonsik Choi[1], Wu Sun[1], Steve Mara[3], Ulrike Seibt[1] and Suzanne E. Paulson[1]

[1] University of California, Los Angeles, Department of Atmospheric and Oceanic Sciences, 405 Hilgard Ave., Los Angeles, California, USA.

[2] University of California, Los Angeles, Fielding School of Public Health, Environmental Health Sciences Department, 650 Charles Young Dr., Los Angeles, California, USA

[3] California Air Resources Board, Research Division, Sacramento, CA, USA

SI 1. Vegetation Characterization and Optical Porosity of Vegetation

Optical porosity of vegetation is defined as the fraction of pore spaces and gaps in the total area of the tree crown profile. High porosity corresponds to low density vegetation and/or large amounts of gaps between trees. The height and optical porosity of the vegetation barriers at the measurement sites was estimated as described below.

We identified large tree canopies for each highway section from the satellite imagery of Google Earth Pro software (Figs. SI1). Satellite images used dated from 2016. Each highway section investigated spans 200 m-100 m in both directions from each target transect, which should cover most contributions from vegetation under both parallel and perpendicular wind configurations. Additionally, locations of the tree canopies were validated against Google Street View images seen from the highways and from the local roads. The identified tree locations were additionally validated in field visits. We did not find any significant misrepresentation of tree objects in Google Earth Pro compared with field observations, indicating the reliability of the geo locational data in Google Earth Pro.

Horizontal dimensions of the trees and their heights with respect to the highway road surface, and distances to the local road section where air sampling were conducted, were measured in Google Earth Pro. We validated the tree heights at the Santa Monica sites using trigonometric methods in the field and found that measurements from Google Earth Pro were within 10% accuracy compared with field values.

(a)

(b)

Fig. SI1 Aerial view and locations of trees at the (a) vegetation barrier (Granville) and (b) combination barrier (Dorchester) transects in Santa Monica (Map source: Google Earth).

Optical porosity (also known as foliage transparency in forestry) of the tree crowns were measured according to a field guide for vegetation structure measurements by the US Forest Service (USFS, 2011). The tree crown as seen by the observer is compared with the images of tree crowns with known density values on a standard Crown Density–Foliage Transparency Card to determine the optical

porosity. Measurements of the optical porosity values of the canopies were conducted in the field near the highway soundwalls using this USFS method (USFS 2011).

We estimated the average heights and optical porosity for vegetation within ± 100 m of the intersection of each transect and the freeways (Figs. SI2). Furthermore, we also calculated an effective optical porosity of the comparable "scene" for the pairs of transects; this is for a height equal to the tallest tree at either transect. As this calculation includes a significant amount of sky, the optical porosity values calculated this way are quite high. In general, it is very difficult to link optical porosity directly with tree species, since the leaf area of a tree species is not a consistent parameter, but depends on the tree stand age and environmental parameters such as water stress, nutrient status, etc. With this significant caveat in mind, Table SI1 shows a very *qualitative* description of the optical porosity of several species identifiable at the measurement sites.

Average optical porosity for each section was calculated by weighting optical porosity of individual canopy by length along the highway direction, and height. Gaps between tree canopies were also accounted for by assigning 100% porosity. We followed these steps in calculating the average optical porosity:

1. Calculate the average height of the trees weighted by their widths. If the height of the tree i is h_i, the width is w_i, and the total length of canopy-covered section is W^* (excluding gap segments), then the average height is

$$\bar{h} = \frac{\sum_i h_i w_i}{W^*}$$

Note that gaps between trees are not considered in the above equation.

2. Calculate the height-weighted average crown density using the average tree height $\bar{h}$ as the threshold. For overlapping trees, crown density (δ) in the overlapping are cannot exceed one. The reason to use crown density (1 – optical porosity) for the averaging instead of optical porosity is that, the sky portion above a tree canopy will be automatically accounted as having zero density this way.

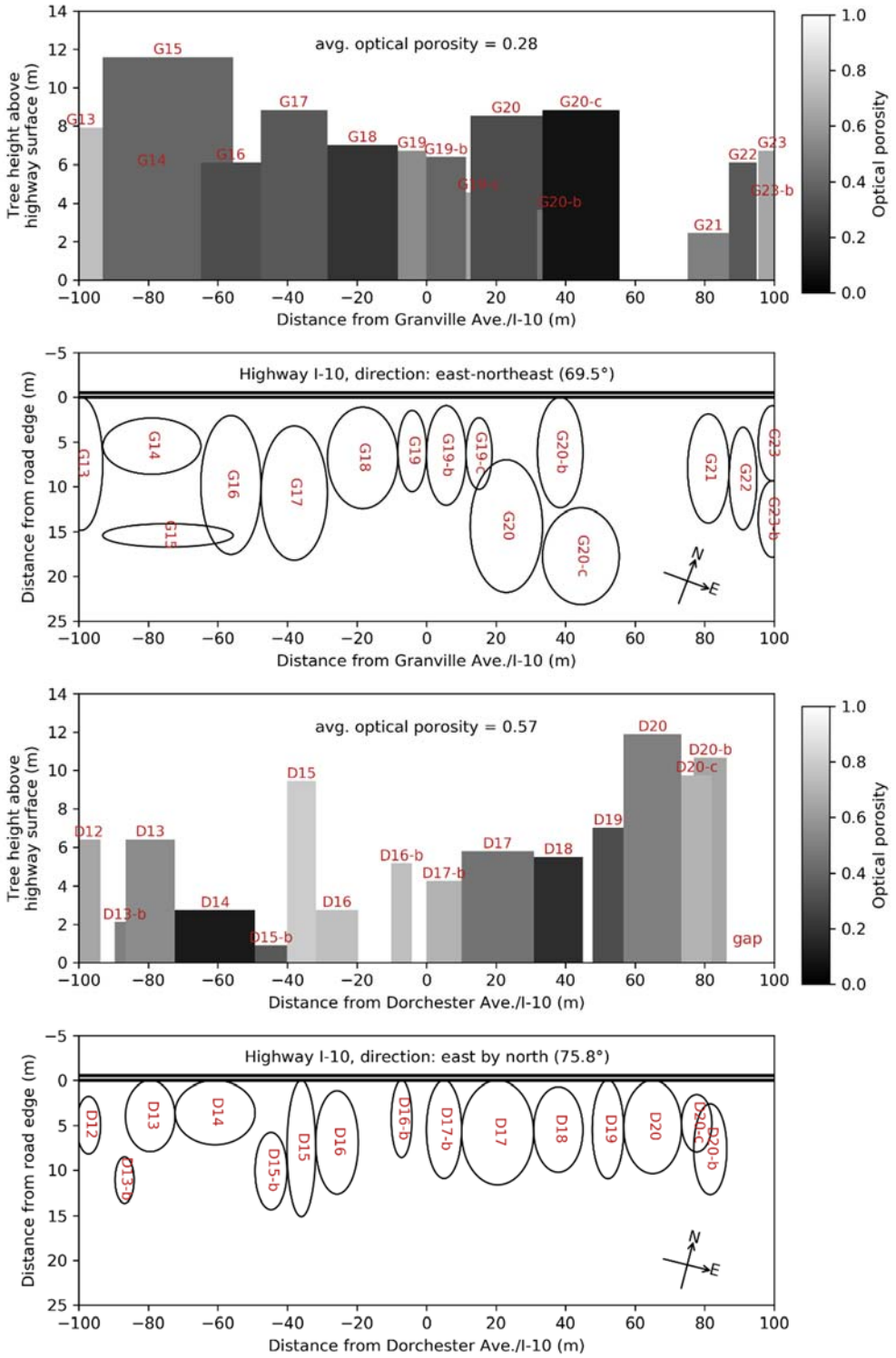

Fig. SI2 Profile view (top panels) and top view (bottom panels) of the tree canopies along (a) vegetation barrier (Granville) and (b) combination barrier (Dorchester) transects in Santa Monica. In the profile view panels,

tree columns are colored coded by the optical porosity. The "average optical porosity" indicates the average at the average height of the tree canopy.

Table SI1. Approximate optical porosity for some representative tree species observed at the study sites in Southern California

Tree species	Optical porosity*
Schinus molle	high
Schinus terebinthifolius	high
Chilopsis linearis	high
Jacaranda mimosifolia	medium
Afrocarpus falcatus	medium
Pinus canariensis	high
Eucalyptus polyanthemos	medium
Cupressus sempervirens	low
Fraxinus uhdei	medium

*High (> 60%), medium (30–60%), low (< 30%). The lower the optical porosity, the denser the tree crown.

The average crown density of the section is

$$\bar{\delta} = \frac{\sum_i h_i w_i \cdot \delta_i}{\bar{h} W}$$

where W is the total length of the section including canopies and gaps (200 m).

3. The average optical porosity is then the reverse of the average crown density on a 0 to 1 scale, i.e.,

$$\bar{\theta} = 1 - \bar{\delta}$$

The average heights and porosities for vegetation within ± 100 m of the intersection of each transect and the freeways at the Santa Monica and Sacramento sites are listed in Table SI2. Figure SI3 shows the effective optical porosity at each site as a function of height.

Table SI2. Average height and average porosity of trees at each location on the primary downwind side, and max height of any vegetation at either of each pair of sites, and the corresponding optical porosity for the max height.

Name	Mean height (m)	Mean optical porosity (dimensionless)	Max height (m)	Mean optical porosity rescaled to max height (dimensionless)
I-10/Granville Ave. (Vegetation only)	7.7	0.28	11.9	0.53
I-10/Dorchester Ave. (combination barrier)	5.9	0.57	11.9	0.79

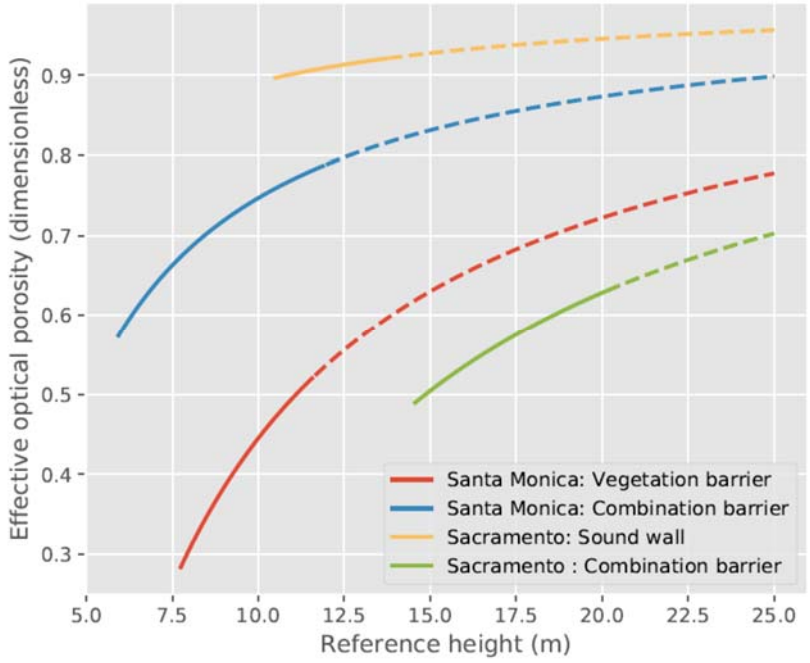

Fig. SI3 Effective optical porosity as a function of height. The solid lines indicate the heights up to the maximum height of any tree in the scene; dotted lines include increasing amounts of clear sky. High porosity corresponds to low tree density and/or gaps between trees.

SI 2. Removal of High-emitting vehicle related spikes

Site-specific distance bins and threshold values were chosen based on the location of local roads and general traffic volume on those roads during the measurement period. All of the transects were selected such that close to the freeway they had minimal traffic, resulting in minimal HEV-related spikes. Therefore, all data collected within the first 40 m from the edge of the freeway were retained. At distances less than 40 m from the edge of the freeway, short-lived spikes observed in the time series were manually removed by identifying HEV related incidents using traffic video from the MMP. With increasing distance from the freeway, sites had arterial roads with heavy traffic. Hence, the thresholds for HEV removal were exponentially decreased as follows. For 40-150 m, 150-300 m, 300-450 m and > 450 m, the threshold was set to 12, 9, 6 and 3 baseline thresholds, respectively. All concentration values above the calculated threshold were replaced by the baseline concentration values to obtain the HEV spike-removed concentration time series.

The usage of a site- and session-specific baseline threshold together with distance based cutoff threshold successfully removed the short-lived HEV related spikes, while retaining the slow varying freeway signal (Fig. SI4). The HEV removal calculations were repeated with several small increments and decrements to the distance bins and threshold values to investigate the sensitivity of the final results to the values chosen in the HEV removal process. No changes were observable in the final results, indicating a low sensitivity.

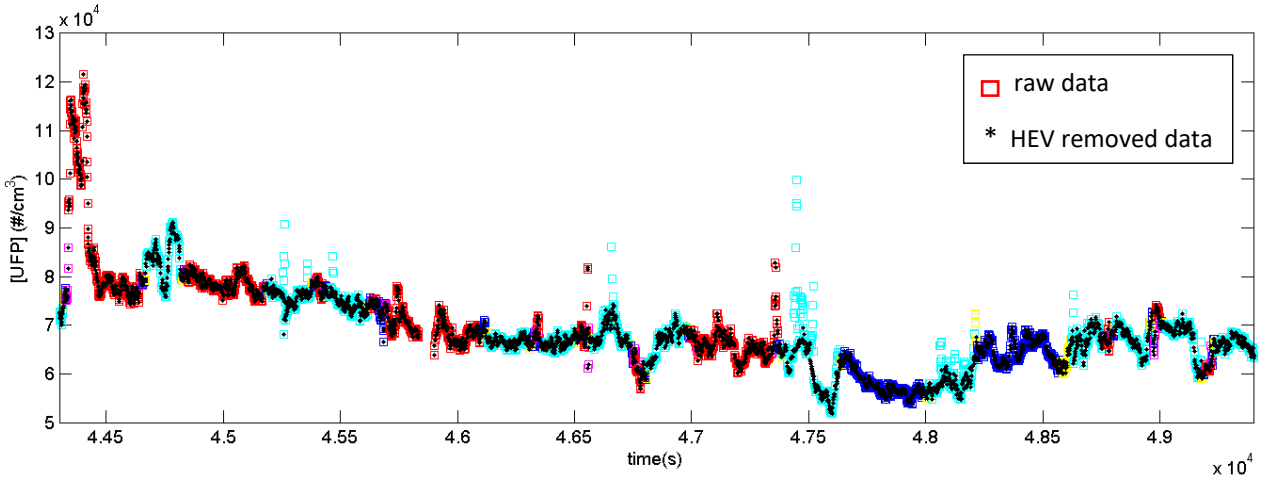

Fig. SI4 An HEV spike removed UFP concentration time series of the Sacramento site. The squares show the raw UFP measurements. Each color represents a distance bin from the freeway;< 40 m (red), 40-75 m

(magenta), 75-120 m (blue), 120-160 m (yellow) and > 160 m (cyan). The squares with black dots show the concentration time series after HEV spike removal.

SI 3. Traffic flow variation at the measurement sites

The freeway traffic flow at each measurement site was calculated as described in Section 3.2. Figure SI5 shows the 30 min mean of the traffic flow in both directions at each measurement transect, together with the standard deviations of the means at the Santa Monica sites. The day-to-day variation in the traffic flows was very small. Averaged over the measurement period and all measurement days, the freeway traffic flow near Granville Ave. was 1.1, 2.5, 5.8 % higher than the freeway traffic flow near Dorchester Ave in the summer, fall and winter sessions, respectively.

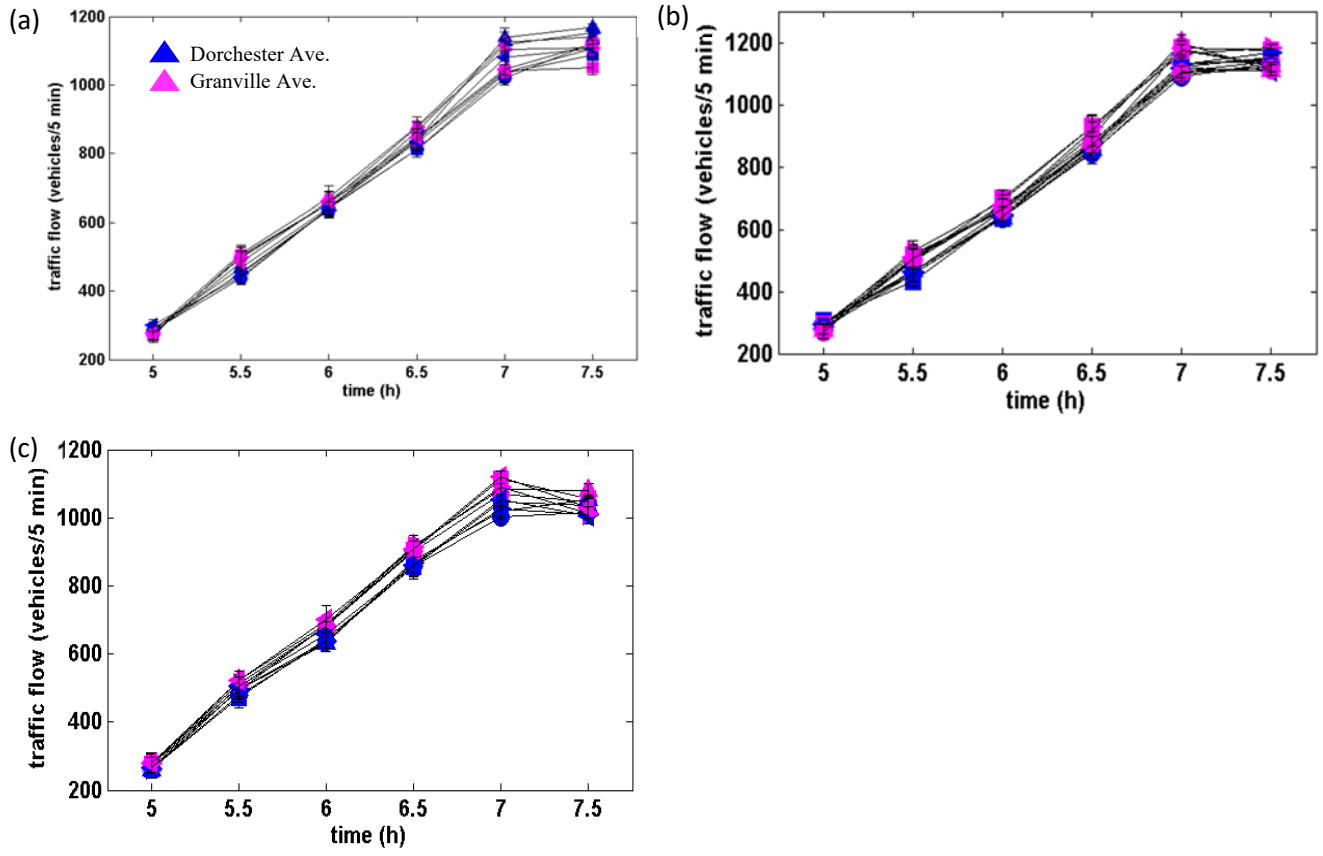

Fig. SI5 The diurnal traffic flow variation on I 10 at Santa Monica site, during (a) summer, (b) fall and (b) winter measurement sessions. The 30 min mean of the traffic flow in both directions at each measurement transect

(color symbols) and the standard deviation of the mean. Different symbols indicate different measurement days.

SI 4. Upwind pollution levels of particulate matter

The number of mobile measurement runs conducted on the upwind side of the freeway was limited to two, due to the limitations on measurement time and mobile platform mileage. The session mean pollution concentration levels of some pollutants on upwind of the freeway are shown below for each transect, when winds were perpendicular to the freeway (Fig. SI6). The measurements that were made approximately 15-80 m from edge of the road was extracted.

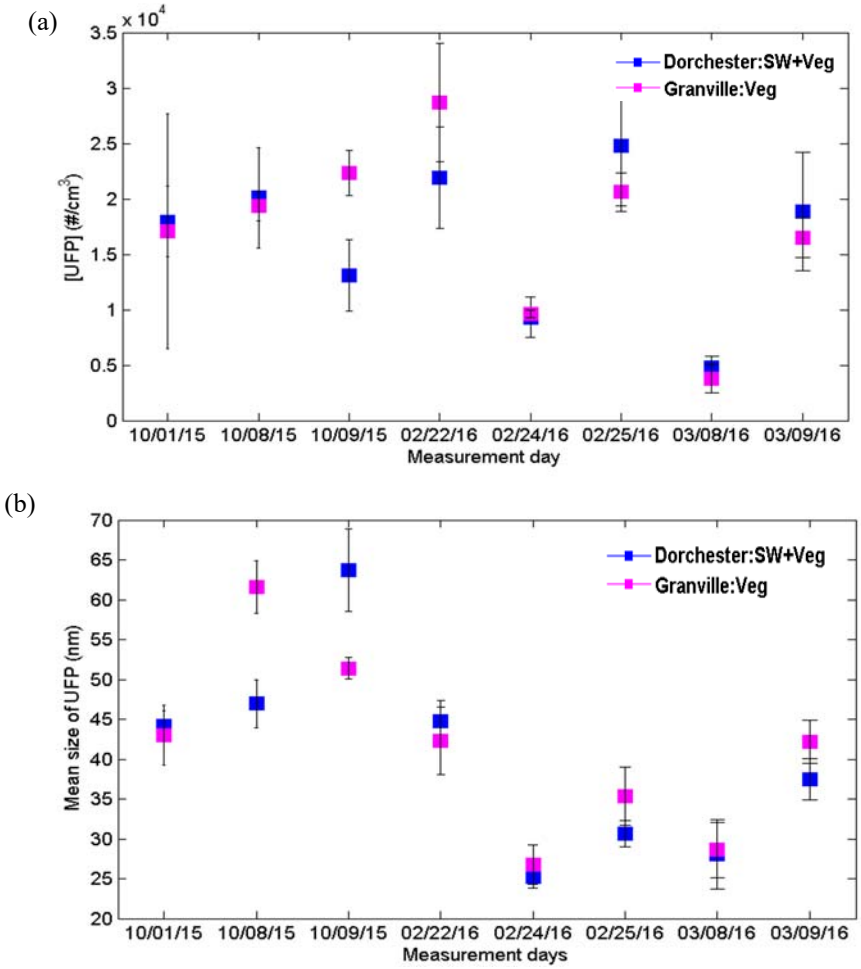

Fig. SI6 The upwind (a) number concentration and (b) mean size of UFP along the two transects at the I-10 Santa Monica site, under perpendicular wind conditions for fall 2015 and winter 2016 measurement session. The session mean concentration is plotted together with the standard deviation.

The upwind site characteristics were different for the two transects. In Santa Monica, the Dorchester street upwind site was situated in a low trafficked residential area while the Grandville street upwind site was downwind of busy arterial road. However, on most days the mean concentration levels at upwind sites were similar, whenever sufficiently large data sets were available for both sites.

SI 5.Continuous Measurements from Passive Samplers: NO and NO_2 Profiles

Figures SI7 and SI8 show [NO] and [NO_2] vs. distance data collected with passive NO_x samplers during the field campaigns at Santa Monica. While there is a pronounced plume from the freeway in the morning (Fig. 3), profiles are indistinct over 24 hours and there is no significant difference between the two barrier configurations in both fall and winter sessions. It could be the result of two factors; at this site the target area is downwind under the stable atmospheric conditions in the mornings, when the meteorology favors very high pollutant concentrations but night time emissions are low, during most the day when emissions are high the target area is upwind of the freeway and intersects some busy surface streets.

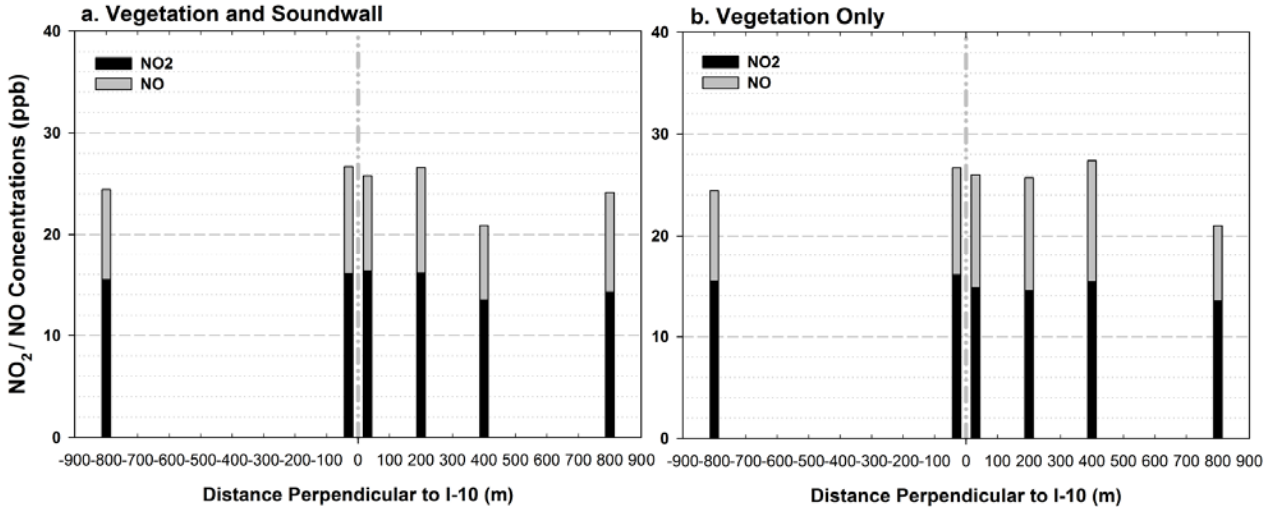

Fig. SI7 NO and NO_2 concentration data collected from Ogawa passive samplers distributed near I-10 in Santa Monica during Sept.-Oct. 2015 along (a) Dorchester Ave. (vegetation and soundwall); and, (b) Granville Ave. (vegetation only).

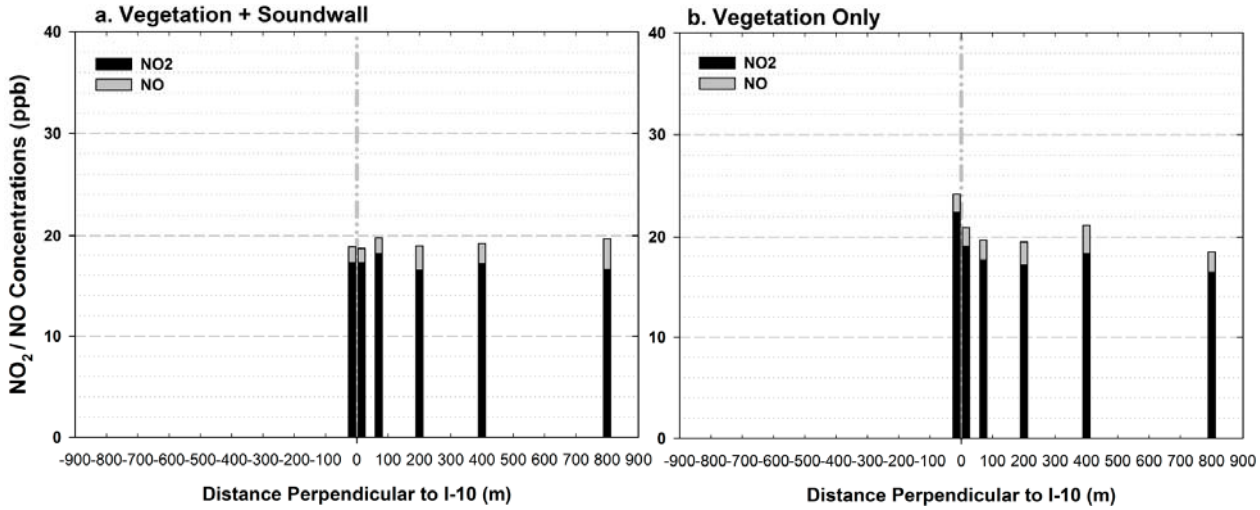

Fig. SI8 NO and NO_2 concentration data collected from Ogawa passive samplers distributed near I-10 in Santa Monica during Feb. - March 2016 along (a) Dorchester Ave. (vegetation and soundwall); and, (b) Granville Ave. (vegetation only).

SI 6.Wind dependence of pollution reduction

The wind speed dependence of the relative reduction of many pollutants such at $PM_{2.5}$, NO (Fig. SI9a and c) was generally similar to that of UFP (Fig.4a), while some pollutants such as PM_{10}, CO (Fig. SI9b and d) showed different patterns.

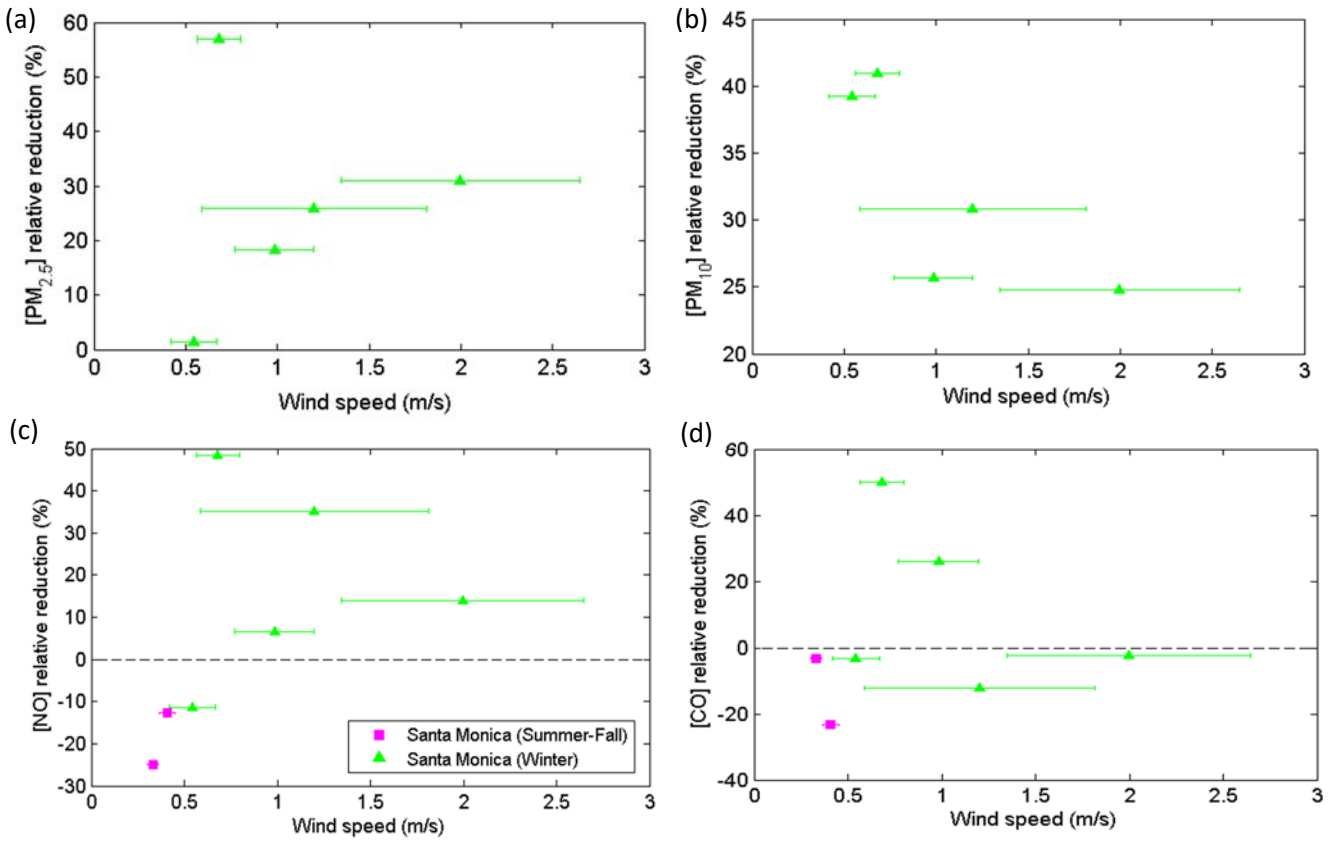

Fig. SI9 The relative reduction of (a) $PM_{2.5}$, (b) PM_{10} (c) NO and (d) CO concentrations by a combination barrier, under downwind conditions, averaged over the first 160 m from the edge of the freeway for Santa Monica site, as a function of the wind speed. Session mean of wind speeds are plotted together with the standard error.

The seasonal average of the mean size of UFP was larger downwind of the vegetation-only barrier in both seasons (Fig. 5). The wind speed dependence of the difference in the mean size of UFP showed a trend decreasing with increasing wind speed, but with much scatter (Fig SI10). This further supports the importance of deposition at lower wind speeds, as the decrease in particle deposition efficiency with increasing wind speed would results in the lower size difference behind the two barriers.

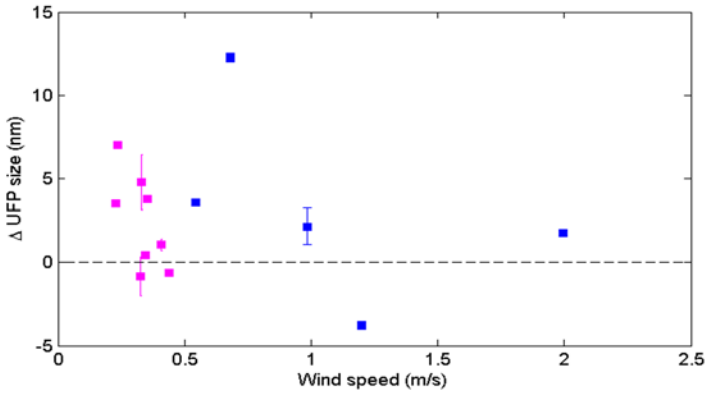

Fig. SI10 The difference of the mean diameters of UFP downwind of the barriers in the summer-fall (pink) and winter (blue) seasons, under downwind conditions, averaged over the first 160 m from the edge of the freeway for Santa Monica site, as a function of the wind speed. Session mean of wind speeds are plotted together with the standard error.

SI 7. UFP Concentration profiles under parallel/near-parallel wind conditions

Figure SI11 shows the average traffic-normalized [UFP] decay profiles under parallel wind conditions at the Santa Monica site. There is no initial rapid decay of [UFP] behind the combination barrier and limited decay behind the vegetation barrier, indicating the low influence of the freeway plume. The benefit of barriers seem very limited under parallel wind conditions in the morning stable atmosphere. The [UFP] behind the combination barrier and the vegetation-only barrier was approximately equal in both summer-fall (Fig. SI11a) and winter (Fig. SI11b) sessions, when averaged over the full length of the transects. However, in both sessions, [UFP] was lower behind the combination barrier at the start of the transects; averaged over the first 80, 60 m from the edge of the freeway, [UFP] was 19, 7% lower in fall and winter, respectively.

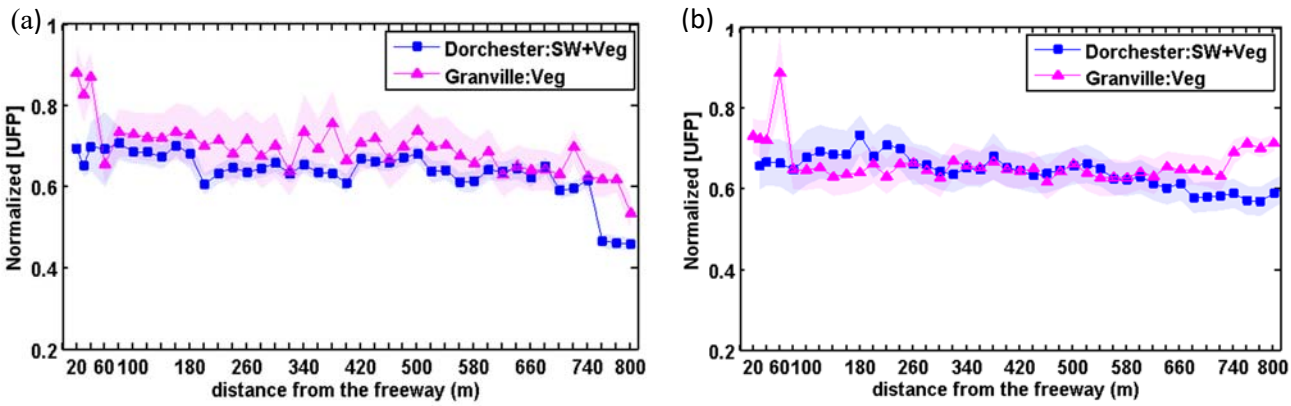

Fig. SI10 The normalized UFP number concentration along the two transects at the I-10 Santa Monica site, under parallel wind conditions for (a) summer-fall 2015 and (b) winter2016 measurement sessions. The traffic-normalized concentration averaged over (a) 6, (b) 4 sessions (line) is plotted together with the standard error of the mean (shaded area).

SI 8. UFP Concentration profiles with absolute concentrations

The UFP concentration profiles previously presented were normalized first by traffic flow and then by daily maximum concentrations to account for the variably different parameters that affect pollution concentrations. Fig. SI12 shows the absolute concentration profiles of UFP number concentration at each of the measurement transect in different seasons.

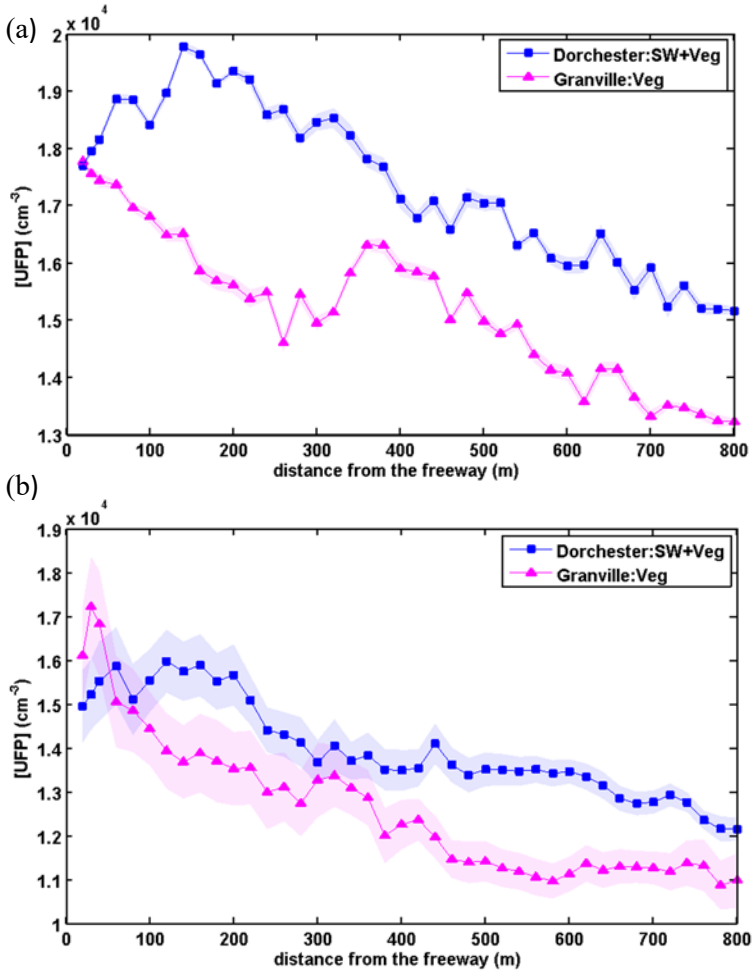

Fig. SI11 The UFP number concentration along the two transects at the I-10 Santa Monica site, under perpendicular wind conditions for (a) summer-fall 2015 and (b) winter2016 measurement sessions. The concentration averaged over (a) 8, (b) 5 sessions (line) is plotted together with the standard error of the mean (shaded area).

SI 9. The sensitivity of UFP Concentration profiles to daily maximum normalization

To account for the daily variations in the urban background, a daily maximum normalization was utilized in developing the session average concentration profiles, as described in section 3.1. The daily maximum concentration of transects was obtained from daily average concentration profiles made from

HEV-removed, wind filtered data averaged at line reference points. Then the daily average concentration profiles of both transects were normalized by dividing all values by the daily maximum concentration. As the choice of the daily maximum was arbitrary, a sensitivity test was performed to investigate the effect of daily maximum normalization on UFP concentration profiles and relative reduction percentages by employing the daily minimum instead of the daily maximum.

Since this normalization procedure was developed to retain the difference between the daily concentration profiles of the two transects, use of either the daily maximum or the minimum resulted in similar session average concentration plots (Figs. SI13 and 14). The relative reduction percentages calculated with the daily maximum and the minimum normalizations were comparable, indicating a low sensitivity of the daily maximum normalization on the barrier comparison results (Table SI3).

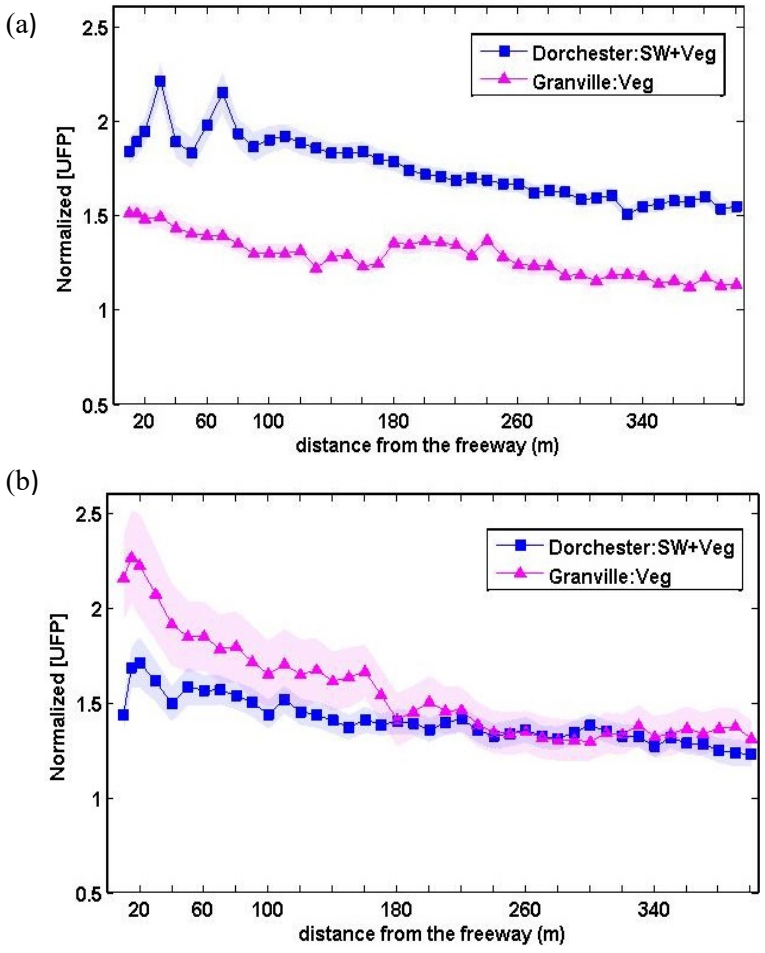

Fig. SI13 The daily minimum normalized UFP number concentration along the two transects under perpendicular wind conditions for (a) summer-fall 2015 and (b) Winter 2016 measurement sessions. The traffic-normalized concentration averaged over (a) 8 and (b) 5 sessions (lines) is plotted together with the standard error of the mean (shaded areas).

Table SI3. Relative reductions[a] (%) of UFPs with daily maximum and daily minimum normalizations

Session	**calm**		**light winds**	
	(wind speed< 0.6 m/s)		**(0.6 m/s<wind speed< 3 m/s)**	
Normalization	*Full*	*160 m*	*Full*	*160 m*
MAX	-24	-27	16	6
MIN	-26	-26	20	9

[a] relative reduction as defined in Section 4.2